Catalysis Today 167 (2011) 56–63

Contents lists available at ScienceDirect

Catalysis Today

journal homepage: www.elsevier.com/locate/cattod

Glycerol acetylation on sulphated zirconia in mild conditions

I. Dosuna-Rodríguez [1], C. Adriany [1], E.M. Gaigneaux [*,1]

Institute of Condensed Matter and Nanosciences (IMCN)–Division "MOlecules, Solids and reactiviTy – MOST" Université catholique de Louvain, Croix du Sud 2/17, B-1348 Louvain-la-Neuve, Belgium

ARTICLE INFO

Article history:
Received 13 May 2010
Received in revised form 9 October 2010
Accepted 3 November 2010
Available online 23 December 2010

Keywords:
SO_4^{2-}/ZrO_2
Glycerol
Esterification
Acetic acid

ABSTRACT

This work focuses on the role of the hydrolysis ratio over the physicochemical properties of sulphated zirconia (SZ) obtained by the sol–gel method. The solids obtained were tested in the esterification of acetic acid diluted in glycerol, the latter being used both as reactant and solvent. The acidic properties of the SZ samples and their performances in the acetylation reaction have been successfully correlated. The recyclability has also been studied: sample SZ-1 (sulphated zirconia prepared with a hydrolysis molar ratio = 1) shows a progressive deactivation in successive tests due to sulphur leaching which induces an activity in the homogeneous phase.

© 2010 Elsevier B.V. All rights reserved.

1. Introduction

The production of first generation biodiesel (fatty acid alkyl esters) has been growing continuously during the last few years. This is principally due to the benefits of biodiesel in comparison with conventional fuels derived from petroleum: it is renewable, biodegradable, non-toxic, and essentially free of sulphurous and aromatic species [1]. First generation biodiesel is generally produced by transesterification of triglyceride processes, with, a side effect, a large amount of glycerol obtained as by-product. With the purpose of making the biofuel industry economically and environmentally viable, this glut of glycerol has to be revaluated [2].

Several solutions are proposed, aiming at either forming new molecules or species [3] or leading to new market opportunities [2]. A possible solution is the etherification of glycerol with tert-butanol and isobutylene [4–6] in order to produce commercial ethers that could be used to decrease the viscosity and the cloud point of biodiesel. Another possibility is the formation of acetals or glycerol carbonates, which can also reduce the viscosity of biodiesel and particle emission [7,8]. Finally, the esterification of short chain carboxylic acids, for example acetic acid with glycerol, in order to form acetylated products is envisaged. This solution leads to the formation of glyceryl monoacetate (MAG), glyceryl diacetate (DAG), and glyceryl triacetate (TAG), whose applications are in the cryogenic industries, the chemical sector of biodegradable polymers and many other uses ranging from cosmetics to food additives (E1518). In addition, the DAG and TAG are good additives for fuels such as biodiesel and gasoline because they improve their viscosity. TAG meets the specifications EN 14214 and ASTM D6751 for the flash point and oxidative stability of carburant. Oxidation stability is required in order to prevent degradation of the fuel, so that it does not decompose into aldehydes, acids or polymers in the presence of peroxides [3,9].

Concerning the esterification of glycerol, inorganic materials functionalized with SO_3H sulphonic groups have attracted much attention: functionalized mesoporous silica-type SBA-15 showed high selectivity and conversion in the acetylation of glycerol. Moreover, this solid could be reused, although a regeneration step is required [10]. Mesoporous silica MCM-41 sulphonated and functionalized with different alkyl chains (methyl, ethyl, propyl and phenyl) presented a good combination between the hydrophobic character of alkyl groups and the acidity of SO_3H species, favouring the selectivity to monosubstituted glycerol in the esterification of lauric and oleic acids. However, the recyclability properties of these materials remain unclear [11–13]. In addition, these solids cannot be applied at the industrial scale due to the high cost of the copolymer involved in their preparation and to the complexity of the functionalization process [3]. Gonçalves et al. [14] compared the different performances of Amberlyst-15, montmorillonite K-10, niobium oxide and zeolite HZSM-5 and H-USY. Amberlyst-15 showed the best catalytic activity in terms of conversion of acetic acid and selectivity to triacetin. Liao et al. [3] compared the behaviour of Amberlyst-15 and Amberlyst-35 ion

* Corresponding author at: Université catholique de Louvain, Institute of Condensed Matter and Nanosciences (IMCN)– Division "MOlecules, Solids and reactiviTy – MOST", Croix du Sud 2/17, 1348 Louvain-la-Neuve, Belgium.
Tel.: +32 10473665; fax: +32 10473649.
E-mail address: eric.gaigneaux@uclouvain.be (E.M. Gaigneaux).

[1] IMCN and MOST are new research entities involving the group formerly known as "Unité de catalyse et chimie des matériaux divisés".

0920-5861/$ – see front matter © 2010 Elsevier B.V. All rights reserved.
doi:10.1016/j.cattod.2010.11.057

exchange resins and HY and HZSM-5 zeolites. In their experiments, the reaction conditions were set to lead to a selective production of triacetin. In these conditions, the Amberlyst-35 could be recycled without any loss of the catalytic activity. The combinations of Starbon® (mesoporous carbon material derived from starch with sulphonic functions) and the use of microwave radiation allowed an almost complete conversion of glycerol (99%) in the presence of acetic acid [15].

Among the various types of solid acids that can be used as esterification catalysts, this work focuses on sulphated zirconia (SZ). Sulphated zirconia finds a large number of applications in industry because of its well-known high acidity [16]: selective isomerisation of hydrocarbons under mild conditions [17], dehydration [18], alkylation [19] or esterification [20], among others. This solid is known as a superacid solid, but this classification is actually not correct, since it has been analysed by Hammett indicators, which are more reliable in the characterisation of liquid substances [21]. The final properties of SZ can be modulated by the synthesis method chosen and the parameters applied. In this work, the sol–gel method is used instead of the classical two step method because of the better anchoring of sulphur species that sol–gel could provide. In addition, the powders obtained by the sol–gel method usually show a larger surface area and the pore size distribution can be varied by different parameters (chemical composition of the alkoxide/solvent synthesis, H_2SO_4/alkoxide and H_2O/alkoxide molar ratios; temperature, reactive addition rate and gel aging time) [22,23].

Various studies have tested sulphated zirconia in several esterification and transesterification reactions carried out in liquid phase [20,24–29]. These reactions were recurrently performed at temperatures higher than 373 K and in the presence of an excess of carboxylic acid. Regarding the recyclability of the solids, studies differ, but in most cases the catalysts gradually lost their activity during the course of test reactions.

In this article we focus on the preparation of SZ solids by the sol–gel method and varying the hydrolysis ratio. The work studies the influence of the latter ratio on the textural, structural and acidic properties, as well as the sulphur content of the samples after the calcination step. The catalytic performances were tested for the acetylation of glycerol in mild conditions, namely working with acetic acid diluted in glycerol, and at a low temperature in order to avoid leaching and to lower the energy requirements. These conditions are opposed to the ones used in the referenced articles, in which glycerol is the limiting reactant and temperature is higher. The stability of the prepared solids in terms of recyclability was studied since some previous works suggested a possible deactivation due to leaching of sulphur species [27]. This work also considers the possibility that the sulphur species could leach away into the reaction medium. In addition the role of these leached species as homogeneous catalyst in the reaction has been studied.

2. Experimental

2.1. Preparation of the catalysts

The catalysts were prepared by one-step sol–gel technique. Sulphuric acid (96%, Merck) was added drop wise to a mixture of zirconium propoxide (70%in 1-propanol, Aldrich) and 1-propanol (>99.5%, Acros Organic) with a concentration of Zr in propanol equal to 1 M and an initial atomic ratio S/Zr = 0.5 under continuous stirring and at room temperature. The sulphuric acid was used both as the sulphating agent and as the catalyst of the polycondensation of the gel. After 1 h under stirring a defined quantity of distilled water was added in order to accomplish the desired H_2O/alkoxide molar ratio named hydrolysis ratio, *H*, which was modulated from 0 to 6. The gels obtained were dried at 393 K for 12 h, and then calcined in air at 833 K for 3 h (heating rate 3.5 K/min). Catalysts are denoted SZ-*H*, where SZ stands for sulphated zirconia and *H* represents the hydrolysis ratio employed.

2.2. Characterisation

N_2-Physisorption experiments were carried out on a Micromeritics Tristar 3000 at 77 K working with relative P/P_0 pressures in the range of 10^{-2}–1.0. The samples were degassed overnight under vacuum (50 mTorr) at 423 K. The specific surface area was calculated from the adsorption isotherm in the 0.05–0.30 P/P_0 range using the BET method. The pore size distribution, mean pore diameter and pore volume were determined by the BJH method (Barret, Joyner and Halenda) exploiting the desorption data. X-ray diffraction (XRD) measurements were performed on the fresh catalysts with a Siemens D5000 diffractometer using the Kα radiation of Cu (λ = 1.5418 Å). The 2θ range was scanned between 5° and 90° at a rate of 0.02 °/s. The sulphur and zirconium contents of the samples were measured by inductively coupled plasma-atomic emission spectroscopy (ICP-AES) on an Iris Advantage apparatus from Jarrell Ash Corporation. XPS analysis was performed on a Kratos Axis Ultra spectrometer (Kratos Analytical, Manchester, UK) equipped with a monochromatized aluminium X-ray source (powered at 10 mA and 15 kV) and an eight channeltron detector. The pressure in the analysis chamber was about 10^{-6} Pa. The pass energy was set at 160 eV for the wide scan and 40 eV for individual spectra. The detection angle was fixed at 0°. In these conditions, the full width at half maximum (FWHM) of the Ag $3d_{5/2}$ peak of a standard silver sample was about 0.9 eV. The following sequence of spectra was recorded: survey spectrum, C 1s, O 1s, S 2p, Zr 3d, and C 1s again, to check the stability of charge compensation as a function of time and the absence of degradation of the sample during the analyses. The C–(C,H) component of the C 1s peak of carbon was fixed to 284.8 eV to set the binding energies. Charge stabilisation was achieved with the help of the Kratos Axis device. Data treatment was executed with the CasaXPS program (Casa Software Ltd, UK), some spectra were decomposed with the least squares fitting routine provided by the software with a Gaussian/Lorentzian (70/30) product function and after a linear baseline subtraction. The O 1s peak was split into two components (O-S and O-Zr) attributed to sulphate species and a Zr–O network of zirconium oxide respectively, without any constraint imposed. The I (S $2p_{3/2}$)/I (S $2p_{1/2}$) intensity ratio was fixed at 2 with an energy difference of 1.18 eV. The I (Zr $3d_{5/2}$)/I (Zr $3d_{3/2}$) intensity ratio was fixed at 1.5, with an energy difference of 2.43 eV [30]. Molar fractions were calculated using normalized peak areas on the basis of acquisition parameters and sensitivity factors provided by the manufacturer. Acidity properties of samples were evaluated by temperature programmed desorption of ammonia (NH_3-TPD). Prior to TPD studies, samples were pre-treated at 833 K for 1 h in a flow of helium gas (Praxair, 60 ml/min). After the pre-treatment, the sample was saturated with 5% anhydrous ammonia gas (Praxair, NH_3–He, 60 ml/min) at 303 K for 1 h. The physisorbed ammonia was flushed out by a flow of He (60 ml/min) at 303 K. NH_3 desorption from 303 K to 833 K (heating rate 10 K/min) was monitored with a mass spectrometer equipped with a quadrupole (Balzers QMC 200). Three temperature zones were arbitrarily associated to the acid sites strength: weak (308–423 K); medium (423–623 K) and strong (623–833 K). The NH_3 desorbed was neutralized in a boric acid solution (20 g/l) and quantified by back titration with a solution of sulphuric acid 0.01 N.

2.3. Catalytic performances measurements

2.3.1. Esterification tests

The esterification reactions were carried out at 328 K and atmospheric pressure in a round bottom flask reactor equipped

with a magnetic stirrer and placed in an oil bath. The acetic acid (puriss. p.a., ACS reagent, ≥99.8%, GC/T, Fluka) concentration was 100 g/l of glycerol (puriss. p.a., ACS reagent, anhydrous, dist., ≥99.5%, Fluka) which corresponds to an initial molar ratio acetic acid:glycerol = 1:82; the catalyst concentration being 6.25 g/l of glycerol. Samples of the reaction medium were analysed by gas chromatography Cp-Sil 8CB with a FID detector, after extraction with 1-heptanol (98%, Sigma Aldrich) using o-xylene (98%, Aldrich) as the internal standard. The activity results are presented in terms of total yield of esters obtained.

The test procedure was as follows: the catalyst was put in the reactor together with the glycerol and the mixture was brought to the reaction temperature. When the temperature was reached, acetic acid was injected. One minute after the injection, a sample was taken and analysed. This result was considered as the original chemical composition of the medium. This process was necessary to exclude the possibility that the catalytic measurements were interfered with the disappearance of acetic acid due to evaporation phenomena during its injection.

Amberlyst-15 was used as a reference catalyst after drying under vacuum at 105 °C. In order to verify the role of the different species participating in the reaction several tests were carried out with: zirconia (ZrO_2 monoclinic, Acros, 98·5%, specific surface area: 64.3 m^2/g), SO_4^{2-} anions as added in the reactor via dissolution in the reaction medium of $(NH_4)_2SO_4$ and H^+ as added in the reactor via H_2SO_4. All these experiment were carried out with equivalent quantities of species as for the SZ-1 sample (Zr and S).

In order to verify the role of acidic properties of the solids over the catalytic performances an additional test was carried out in the presence of SZ-3 sample, but varying the mass of solid added (~0.35 g instead of 0.25 g), so that the reaction was done with the same number of acid sites as with the SZ-1 sample. This test is named SZ-3*.

2.3.2. Distribution of esters

A specific test was carried out in order to discover whether the origin of the preferential formation of one product over another was thermodynamic or catalytic. The test was performed at the same temperature and pressure as the catalytic tests. 1.57 ml of a mixture of esters (Monoacetin, 40%, Acros) were added to 40 ml of glycerol, in the presence of 0.25 g of SZ-1 catalyst. For comparison, the same test is performed in the absence of catalyst (blank reaction).

2.3.3. Leaching tests

The leaching tests were performed in the same conditions as the catalytic tests except for the catalyst concentration (5 g/l of glycerol) and the temperature (338 K). S and Zr contents of the filtered liquid media (13 mm, PTFE syringe filter (0.45 μm), VWR) were analysed by ICP-AES technique. Two types of tests were carried out: one in the presence of glycerol only and the other one in the presence of the reaction mixture (acetic acid and glycerol).

2.3.4. Recyclability tests and homogeneous test

The recyclability tests were carried out in the same conditions as the catalytic tests: after 16 h reaction time, the catalyst was separated from the liquid medium by centrifugation and then put in a fresh reaction medium without further pre-treatment. The used liquid medium (LM) was filtered and kept in the reaction conditions. Samples of the reaction medium were analysed periodically, as it was done with the SZ. The liquid medium was also analysed by ICP technique in order to detect the leached species.

Table 1
Textural properties of SZ samples.

Sample	BET surface area (m/g)	Pore volume (cm^3/g)	Pore diameter average (Å)
SZ-0	9	0.02	221
SZ-1	68	0.03	24
SZ-3	31	0.04	48
SZ-6	139	0.20	51

3. Results and discussion

3.1. Textural properties

The surface area, total pore volume and average pore diameter are given in Table 1. All the solids obtained were mesoporous. The SZ-0 sample exhibited a very low specific surface and an average pore diameter, while the SZ-6 presented the highest specific surface area. It can be observed that there is no linear correlation between the textural properties of the samples and the variation of the hydrolysis ratio.

3.2. Structural properties

The XRD patterns of SZ samples are shown in Fig. 1. It is important to verify that the metastable tetragonal phase (T), known to be catalytically active [31], is obtained at the expense of the monoclinic phase. The characteristic peak of the monoclinic phase, located at 28.2°, relative intensity of 100% is always totally absent on the collected diffractograms, as well as the one located at 24.0°. The single peak observed at approximately 30°, between the position of the characteristic peaks of the monoclinic (31.5°) and of the tetragonal (30.2°) phases, is attributed solely to the tetragonal phase. Regarding these results, we may conclude that only the tetragonal phase of zirconia is present. However, the presence of amorphous zirconia material cannot be excluded, especially for SZ-3 and SZ-6 which show a broad band around 30°. The amount of amorphous phase could decrease from SZ-6 to SZ-3 and be almost absent for SZ-1.

The diffractogram of SZ-0 sample indicates the presence of a crystalline tetragonal phase developed from an amorphous phase. The rise of the hydrolysis ratio (H) thus clearly causes a stabilisation of the amorphous phase with regard to the tetragonal phase. As a counterpart, it is observed that a lower value of the hydrolysis ratio favours the formation of the tetragonal phase, and that in no case the monoclinic phase is formed.

3.3. Bulk chemical composition

The results of the bulk chemical composition are presented in Table 2. All samples were prepared with a S/Zr initial molar ratio equal to 0.5 (8.6 wt% S) because this ratio leads to an optimal specific surface area/content of S and allows a maximum effective concen-

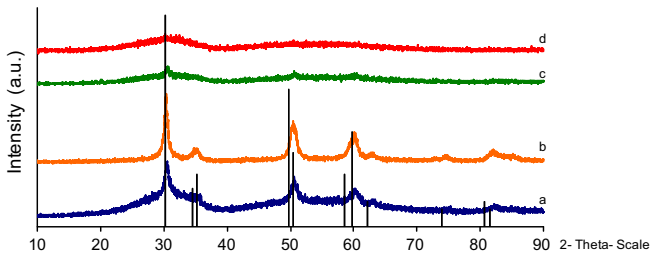

Fig. 1. XRD patterns of sulphated zirconia. (a) SZ-0, (b) SZ-1, (c) SZ-3 and (d) SZ-6. Vertical lines indicate the position of diffraction reflects corresponding to the tetragonal phase and their relative intensities.

Table 2
Bulk chemical composition analysed by ICP and S/Zr final molar ratio.

Sample	S content (wt%)	Zr content (wt%)	S/Zr final molar ratio
SZ-0	8.30	51.26	0.46
SZ-1	6.24	56.93	0.31
SZ-3	7.69	50.80	0.43
SZ-6	7.54	50.00	0.43

tration of sulphur in the final catalyst [32]. It appears that all our samples show a lower S/Zr molar ratio than the nominal one. This is due to sulphur losses, likely during the calcination steps presumably as SO_x. As it can be seen in Table 2, the sulphur content of the samples is included in an interval between 6.2 and 8.3 wt%.

3.4. Surface chemical composition

XPS analyses were performed for all samples to verify the presence of sulphate species and determine the S/Zr final molar ratio at the surface. The results are presented in Table 3. No impurities were found, except the carbon contamination due to the analysis itself. All samples exhibit a lower S/Zr final molar ratio on the surface than in the bulk. This is a typical phenomenon obtained for all the samples synthesized by sol–gel and calcined.

All samples show the peak associated to the S $2p_{3/2}$ (binding energy = 169.4 eV), which confirms the presence of sulphur with an oxidation state + VI, which is expected for sulphate groups at the solid surface. Moreover, any reduction reaction associated with solvent (alcohol) and the alkoxide decomposition has been avoided by the calcination step in air [23].

Regarding the 1s spectrum of the oxygen (Fig. 2), two components can be distinguished: the first at 530.3 eV, corresponding to the oxygen in the network of zirconium oxide and the second, located at 532.1 eV, attributed to oxygen involved in sulphated species [33,34]. It can be noticed that the intensity of the peak located at 532.1 eV becomes more intense when the S/Zr final molar ratio of the surface increases, indicating that a larger number of oxygen atoms are bound to sulphur atoms. This is in agreement with the experimental data in Table 3, where the surface SO_4/Zr is seen to increase when the surface ratio S/Zr increases.

The binding energies of Zr peaks $3d_{3/2}$ and $3d_{5/2}$ of zirconium oxide are typically 182.2 eV and 184.6 eV [33,35]. A shift of 0.7 eV to higher energies is observed for our samples, indicating the electron attracting effect of sulphate groups on the surface Zr species [33].

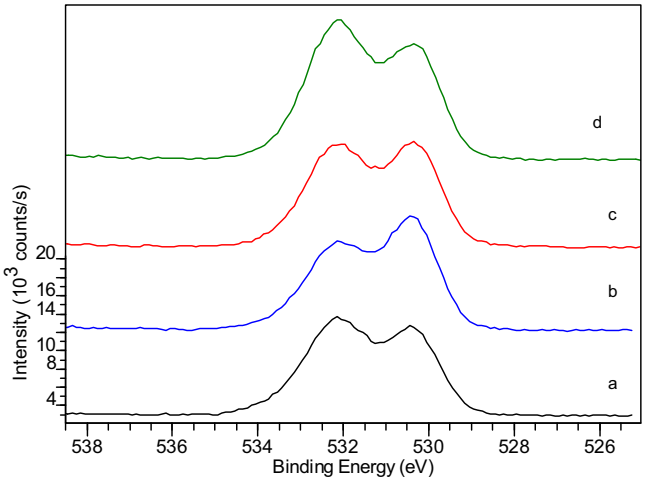

Fig. 2. O 1s XPS spectra of the different samples. (a) SZ-0, (b) SZ-1, (c) SZ-3 and (d) SZ-6.

3.5. NH_3-TPD measurements

NH_3-TPD results obtained for the various catalysts are shown in Table 4. The similarity of the maximal desorption temperatures indicates that the distribution of acid sites strength for all samples is quite similar and thus independent of *H*. SZ-6 exhibits the largest proportion of stronger acid sites in spite of its lowest proportion of weak acid sites. It can be noticed that *H* slightly influences the proportion of weak acid sites in the following way: the higher the *H*, the lower the proportion of weak acid sites. Regarding the total acidity, samples can be sorted as follows SZ-6, SZ-1, SZ-3 and SZ-0, SZ-6 being the most acidic catalyst. If the acid site density (μmol NH_3/m^2) is plotted (Fig. 3), it clearly turns out that values of $H = 1$ and $H = 6$, presenting the highest total number of acid sites, also show the lowest acid site density.

If we report the number of acid sites or, in other words, the number of NH_3 molecules desorbed, to the sulphur content of the surface measured by XPS, we obtain the results given in the last column of Table 4. The values of SO_4^{2-}/NH_3 are closer to 1 for samples SZ-1 and SZ-6 than for SZ-0 and SZ-3. This can be interpreted as follows: the polynuclear sulphate groups represent a single acid site. Consequently we can claim that a higher specific surface area favours the spacing of the sulphate groups, leading to less dense, more accessible and a larger number of total acid sites.

Table 3
Molar ratios determined by XPS and binding energies.

Sample	S/Zr	C/Zr	O_{ZrO_2}/Zr	O_{SO_4}/Zr	Zr $3d_{5/2}$ (eV)	S $2p_{3/2}$ (eV)	O 1s (eV)	
							O-Zr	O-S
SZ-0	0.38	1.170	1.095	2.006	182.9	169.4	530.3	532.1
SZ-1	0.29	0.928	1.277	1.490	182.9	169.4	530.3	532.1
SZ-3	0.37	0.878	1.237	1.727	182.9	169.4	530.3	532.1
SZ-6	0.43	0.771	1.218	2.039	182.9	169.4	530.3	532.1

Table 4
Acidity of SZ samples.

Sample	Maximal desorption temperature (K)	Total acid sites mol NH_3/g	Distribution of acid sites strength			mol SO_4^{-2} (XPS)/mol NH_3 (TPD)
			Weak (%)	Medium (%)	Strong (%)	
SZ-0	399	621	41.9	47.4	10.6	3.70
SZ-1	406	1450	41.5	47.6	10.9	1.27
SZ-3	405	1046	37.2	50.7	12.0	2.17
SZ-6	380	1896	35.6	48.1	16.3	1.35

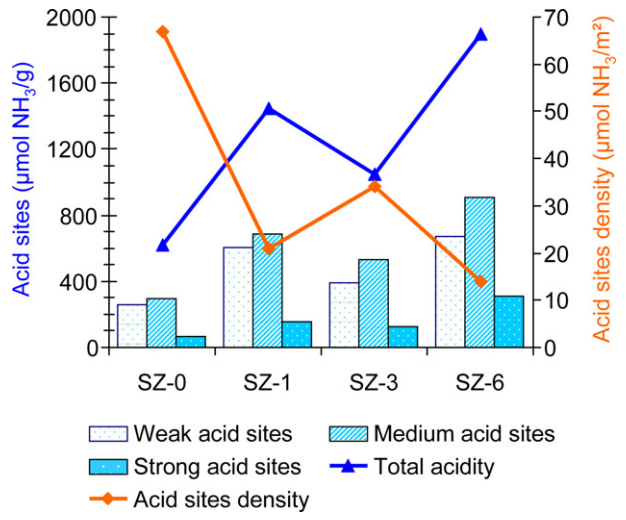

Fig. 3. Acidic properties of the SZ samples, total acidity and acid sites density.

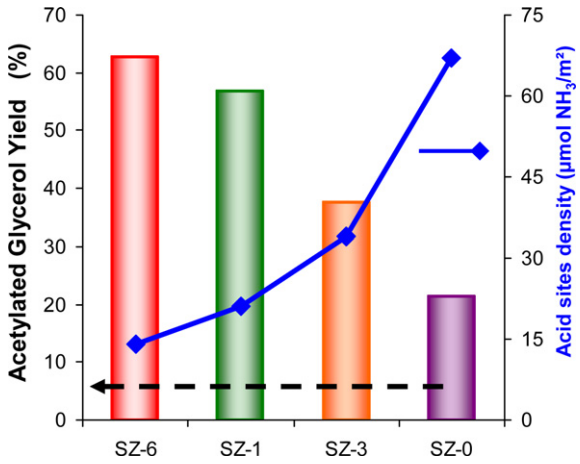

Fig. 5. Acetylated glycerol yield (bar graph, left axis) at 24 h reaction time vs. acid site density of SZ samples (rhombus line, right axis).

3.6. Catalytic performances

3.6.1. Esterification tests

Fig. 4 presents the acetylation yield measured during the blank and the catalytic tests. When the reaction was carried out in the absence of catalyst, the final yield was about 20%, likely due to the activity of the acetic acid protons. Depending on the catalyst added, this reaction is accelerated in different ways. SZ-0 sample does not lead to any improvement, maybe due to the low surface area exhibited. The use of SZ-3, SZ-1 and SZ-6 samples resulted in total acetylation yields of 38%, 57% and 63% respectively, after 24 h of reaction. Amberlyst-15 was used as reference catalyst; after 20 h of reaction the conversion of acetic acid obtained was equal to 95% and the acetylation total yield was close to 80%. This may be reasonably regarded as the equilibrium point of the reaction.

The final acetylation yield of a 24 h reaction test carried with ZrO_2 monoclinic was equal to 20% indicating that non-sulphated zirconia is inactive in this reaction. The use of SO_4^{2-} anion resulted in a total acetylation yield equal to 10%. While H_2SO_4 is used with an equivalent quantity of S species as when SZ-1 solid is used, the equilibrium point of the reaction is achieved in 5 h. This shows that only the protons participate in the improvement of the catalytic performances.

Taking into account the previous characterisation results, we can clearly observe that the catalytic activity is independent of the structural properties of the solid: while SZ-6 is amorphous and SZ-1 is totally stabilised in the tetragonal phase of zirconia, both solids show comparable final acetylation yields. The sole difference found for these samples was the mechanical resistance to attrition during the test, which was higher for the SZ-1 sample than for SZ-6. All the catalysts showed a similar sulphur bulk content, so this parameter can neither be the main parameter influencing the catalytic performances developed in the esterification reaction. Regarding Fig. 4 we observed that the total number of acid sites participating in the reaction does not explain the different activities of the solids, as SZ-1 test and SZ-3* test did not give similar performances, even if the number of total acid sites involved in the esterification was the same. While comparing the final acetylation yield of the reaction with the density of acid sites (Fig. 5) a clear relation is observed: the lower the acid site density, the higher the catalytic activity.

Assuming that the nucleophilic attack by hydroxyl group of the alcohol onto the adsorbed acetic acid over the surface of the catalyst is the determining rate in the esterification reaction [36], this could be explained as follows. The acetic acid molecules adsorbed on the isolated acid sites could present a lower steric hindrance to approach of glycerol than the acetic acid molecules adsorbed on very close acid sites.

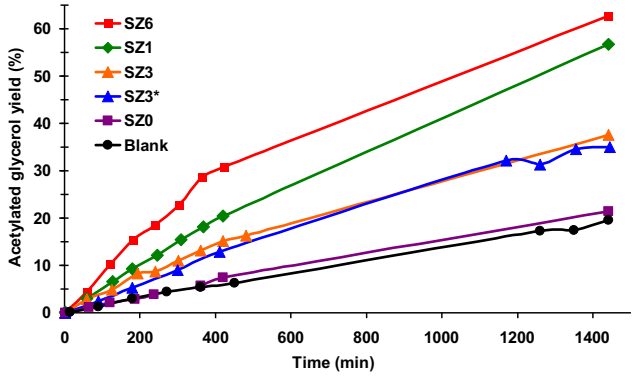

Fig. 4. Total yield in ester profiles of SZ samples during glycerol acetylation. Reaction conditions: reaction temperature: 328 K; catalyst weight: 250 mg/40 ml glycerol; acetic acid concentration = 100 g/l.

3.6.2. Ester distribution

Regarding the distribution of esters developed by each catalyst, no remarkable differences are noticed (Table 5); as the distribution of esters is determined by the equilibrium of the reaction, depending on the reactants concentrations and the temperature and it is not influenced by the catalyst used. It can be claimed that the only role of the catalyst is to accelerate the reaction toward the equilibrium. In the conditions applied, the major product of the reaction was the MAG (with 90% 1-MAG and 10% 2-MAG). The yield to DAG was always lower than 2% (with 70% 1-3DAG and 30% 1-2DAG). In these conditions the formation of TAG was never observed.

Table 5
Total acetylation yield and mole fractions (in percent). Esters produced after 24 h.

Sample	Total acetylation yield (%)	Distribution molar of esters	
		MAG	DAG
Blanc	19.5	99.8	0.2
SZ-0	23.2	99.4	0.7
SZ-1	54.0	98.9	1.2
SZ-3	36.5	99.0	1.0
SZ-6	62.1	98.3	1.7
Amberlyt-15	~80	98.0	2.0

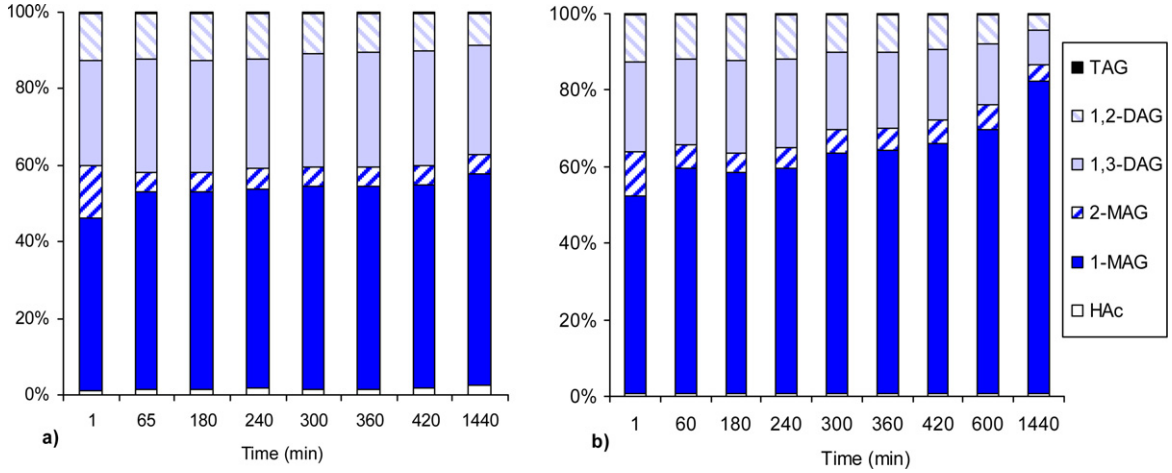

Fig. 6. Distribution of esters test. (a) Blank, (b) test carried out with SZ-1. Reaction conditions: reaction temperature: 328 K; catalyst weight: 250 mg/40 ml glycerol; monoacetin, 40%, concentration = 32.4 g/l glycerol.

As shown in Fig. 6 when starting from the acetin mixture, the concentration of esters other than 1-MAG progressively decrease, while that of 1-MAG increases. This tendency is more pronounced for 2-MAG. When a catalyst (SZ-1) was added to the mixture, this rearrangement is accomplished faster. This demonstrates that the most stable ester in our reaction conditions is 1-MAG, and that the catalyst does not influence the distribution of produced esters.

3.6.3. Leaching tests

The insolubility of the catalysts in the solvent and in the reaction medium, as well as their tendency to leach sulphates, is shown in Fig. 7. Fig. 7a and b represents loss of S and Zr in wt% of the initial sulphur and zirconium present in the solid. In Fig. 7c, the S/Zr molar ratio determined for the liquid media is compared with the S/Zr initial molar ratio. All samples, except SZ-6, show losses lower than 5% for each element. However, the S/Zr molar ratios calculated for the liquid media indicate a significant preference of sulphur leaching. In the case of SZ-6 sample, the leaching values are the highest but the S/Zr molar ratio calculated for the liquids remains quite low. The presence of solid particles in suspension was suspected and verified by means of optical microscopy. We can thus conclude that SZ-6 exhibited a low mechanical resistance and it was divided in fine particles smaller than the filter threshold during the insolubility test.

3.6.4. Recyclability tests and homogeneous tests

Recyclability tests and homogeneous catalysis tests were conducted with the SZ-1 sample. Both SZ-1 and SZ-6 presented good performances in the catalytic reaction but only the SZ-1 sample underwent additional studies as recyclability test. This sample was chosen because of its high activity, and its better mechanical resistance compared to SZ-6 which presented a very low mechanical resistance (during the catalytic test SZ-6 was divided in fine particles which complexified the filtration and consequently the recuperation process).

The results regarding the recyclability tests carried out with the reused SZ-1 solid are shown in Fig. 8a. It can be observed that in the first run the total acetylation yield of the solid is very close to the standard test that confirms repeatability of the tests. The activity developed in the second use of the sample is lower but still remains higher than for the blank reaction. In the successive runs, the activity drops at every reuse of the catalyst. The latter is totally deactivated at the 4th esterification run since the slope of the catalyzed reaction is the same as for the reaction carried out without adding a catalyst. This deactivation is interpreted to occur in consequence of sulphur leaching from the surface of the solid which was quantified by ICP-AES (Table 6) showing that there is a preferential leaching of sulphur species. The quantity of sulphur leached is the more important at the first run and corresponds to a loss of 2.9 wt% of the initial sulphur present (corresponding to 100 wt% of S). This value is lower than the one corresponding to the solubility test due to the lower temperature applied. However, this leaching does not bring a total loss of activity. The solid is indeed still active during the second run, indicating the persistence of sulphates attached to the surface. Unfortunately, these remaining species are not more resistant to leaching than those leached in the 1st run as they also got

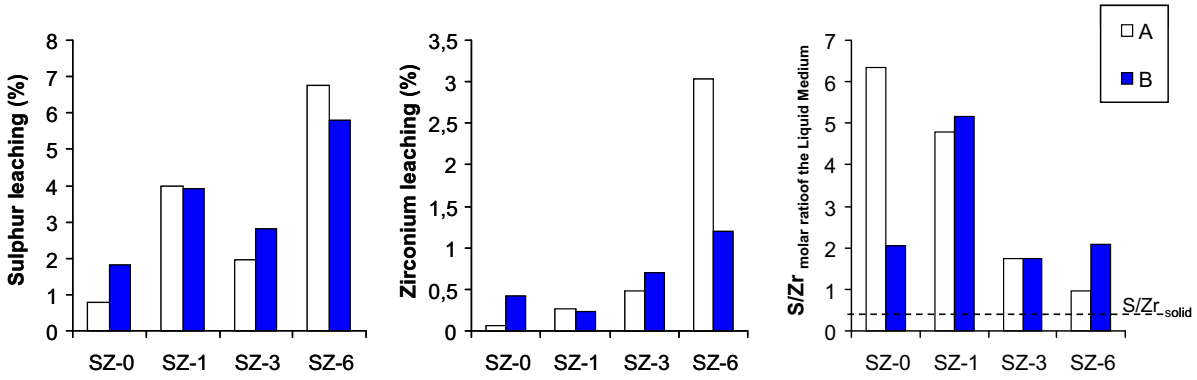

Fig. 7. Leaching of species (a) S and (b) Zr in relative percent (compared to the initial content). (c) S/Zr molar ratio in the treated liquid medium compared to the nominal bulk S/Zr molar ratio (horizontal line). (A) Test carried out in glycerol and (B) tests carried out with glycerol and acetic acid.

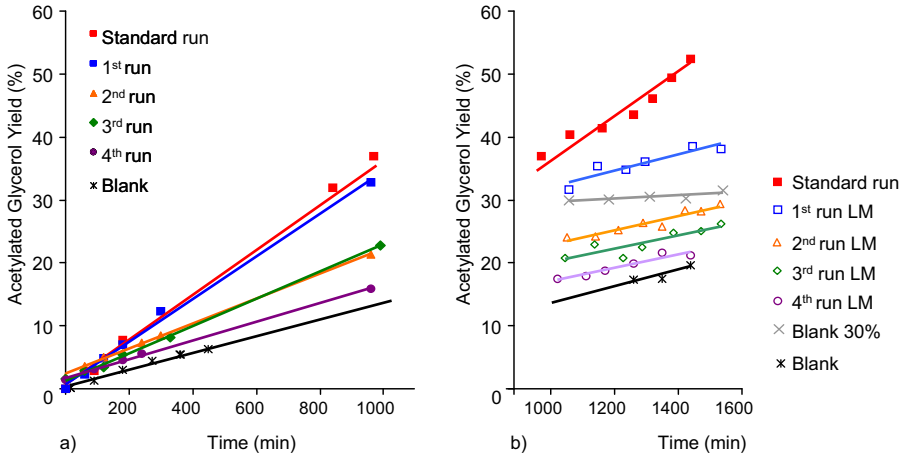

Fig. 8. (a) Recyclability test performed with SZ-1 sample is shown. Reference lines: the activity of one standard test "Standard run" and the blank reaction "Blank". "N-run" stands for the tests carried out in presence of the solid. b) Reference lines: "Standard run" (carried out in presence of the SZ-1 sample), "Blank" and "Blank 30%" which correspond to the activity of the non catalyzed reaction after achieved an acetic acid conversion close to 30%. "n-run LM (Liquid Media)" stands for the activity shown by the liquid phase after its separation from the solid.

Table 6
Concentration of leached species in the filtered liquid medium after the recyclability tests.

	[S] (ppm)	[Zr] (ppm)	S/Zr
1st run LM	7.9	9.7	2.30
2nd run LM	3.1	6.1	1.45
3rd run LM	1.5	3.3	1.26
4th run LM	1.7	6.5	0.74

removed from the solid in the successive runs, leading to impoverish the sulphur content at the surface of the catalyst and to its deactivation.

In order to verify if the sulphur species leached at each run of the recyclability test, could act as a catalyst in homogeneous phase, the activity of the filtered liquid medium (LM) has been studied. As we can see in Fig. 8b, the liquid medium filtered from the first use of the solid (1st run LM) exhibits a lower activity than that obtained if the catalyst is maintained in the reaction, (Standard run), but clearly higher than the blank test (Blank 30%). In the successive tests, the slope of the evolution of the acetylation yield measured for the liquid medium decreases, reaching values close to those obtained for the blank reaction. This can be explained by the concentration of sulphur species in the liquid medium. In the first test this concentration is the highest, as it is generated by the catalyst still very rich in sulphur and leads to an activity in homogeneous phase. In the next runs, the concentration of sulphur in the liquid decreases as generated by solids already impoverished. The catalytic effect of sulphur species in the liquid is thus lower and does not lead to a remarkable improvement of the yield compared to the blank. We suspect that these sulphur species removed from the solid to the liquid as sulphuric acid as proposed by Suwannakarn et al. [27].

4. Conclusions

This study confirms that the physicochemical properties of sulphated zirconia obtained by sol–gel method can be modified by the hydrolysis ratio applied. No linear correlation between the textural and structural properties and the hydrolysis ratio could be found. However, we can state that a lower *H* favours the crystallisation of zirconia in the tetragonal phase which enhances the mechanical resistance of the samples. The acid sites density of the samples has been successfully correlated to the activity exhibited in the esterification reaction: the lower the acid sites density, the more accessible the acid sites and the higher the activity. Independently of *H*, the catalysts showed approximately the same strength distribution of acid sites. The analyses of the filtered liquid medium have shown that a preferential leaching of sulphur occurs during the tests. This leaching is present in every esterification run, as we could observe with the recyclability test of the SZ-1 catalyst: even in soft conditions, the sample is fully deactivated after 4 esterification tests and cannot be directly reused. The deactivation of the samples is apparently due to the continuous leaching of sulphur species. These leached species were able to catalyze the reaction in homogeneous phase depending on their concentration.

Acknowledgements

The authors acknowledge the financial support from the "DGTRE, Région Wallonne" for the project "FuturEnergy-LIGNOFUEL" (Convention number 716721). The research group is also involved in the "INANOMAT" IUAP program (Service Public Fédéral de Programmation Scientifique, Belgium) and in the COST D41 Action (European Science Foundation).

References

[1] F.R. Ma, M.A. Hanna, Bioresour. Technol. 70 (1999) 1.
[2] D.T. Johnson, K.A. Taconi, Environ. Prog. 26 (2007) 338.
[3] X. Liao, Y. Zhu, S. Wang, Y. Li, Fuel Process. Technol. 90 (2009) 988.
[4] K. Klepáčová, D. Mravec, M. Bajus, Appl. Catal., A 294 (2005) 141.
[5] K. Klepáčová, D. Mravec, A. Kaszonyi, M. Bajus, Appl. Catal., A 328 (2007) 1.
[6] H. Noureddini, W.R. Dailey, B.A. Hunt, Chem. Biomol. Eng. Res. Publ. (1998) 232.
[7] B. Delfort, I. Durand, A. Jaecker, T. Lacome, X. Montagne, F. Paille, US Patent 6890364.
[8] J. Delgado Puche, Procedure to obtain biodiesel fuel with improved properties at low temperature US Patent 07637969.
[9] R.L. McCormick, T.L. Alleman, M. Ratcliff, L. Moens, R. Lawrence, Survey of the Quality and Stability of Biodiesel and Biodiesel Blends in the United States in 2004, NREL/TP-540-38836, National Renewable Energy Laboratory, Golden, CO, 2005 (October).
[10] J.A. Melero, R. van Grieken, G. Morales, M. Paniagua, Energy Fuels 21 (2007) 1782.
[11] I. Díaz, C. Marquez-Alvarez, F. Mohino, J. Perez-Pariente, E. Sastre, J. Catal. 193 (2000) 295.
[12] I. Díaz, F. Mohino, J. Pérez-Pariente, E. Sastre, Appl. Catal., A 242 (2003) 161–169.
[13] I. Diaz, F. Mohino, T. Blasco, E. Sastre, J. Perez-Pariente, Microporous Mesoporous Mater. 80 (2005) 33.
[14] V.L.C. Gonçalves, B.P. Pinto, J.C. Silva, C.J. Mota, Catal. Today 133–135 (2008) 673.
[15] R. Luque, V. Budarin, J. Clark, D. Macquarrie, Appl. Catal., B 82 (2008) 157.
[16] G.D. Yadav, J.J. Nair, Microporous Mesoporous Mater. 33 (1999) 1.
[17] A. Sassi, J. Sommer, Appl. Catal., A 188 (1999) 155.
[18] S. Chokkaram, B.H. Davis, J. Mol. Catal. A: Chem. 118 (1997) 89.
[19] R.B. Gore, W.J. Thomson, Appl. Catal., A 168 (1998) 23.
[20] D.E. López, J.G. Goodwin Jr., D. Bruce, S. Furuta, Appl. Catal., A 339 (2008) 76.

[21] A. Corma, Curr. Opin. Solid State Mater. Sci. 2 (1997) 63.
[22] L. Ben Hamouda, A. Ghorbel, F. Figueras, 12th ICC, Stud. Surf. Sci. Catal. 130 (B) (2011) 971.
[23] S. Melada, S.A. Ardizzone, C.L. Bianchi, Microporous Mesoporous Mater. 73 (2004) 203.
[24] T.A. Peters, N.E. Benes, A. Holmen, J.T.F. Keurentjes, Appl. Catal., A 297 (2006) 182.
[25] A.A. Kiss, A.C. Dimian, G. Rothenberg, Adv. Synth. Catal. 348 (2006) 7.
[26] J. Ni, F.C. Meunier, Appl. Catal., A 333 (2007) 122.
[27] K. Suwannakarn, E. Lotero, J.G. Goodwin, C. Lu, J. Catal. 255 (2008) 279.
[28] J. Jitputti, B. Kitiyanan, P. Rangsunvigi, K. Bunyakiat, L. Attanatho, P. Jenvanitpanjakul, Chem. Eng. J. 116 (2006) 61.
[29] C.M. Garcia, S. Teixeira, L.L. Marciniuk, U. Schuchardt, Bioresour. Technol. 99 (2008) 6608.
[30] J.F. Moulder, W. Stickle, P. Sobel, K. Bomben, Handbook of X-Ray Photoelectron Spectroscopy, Perkin–Elmer Corporation, Eden Prairie, 1992.
[31] D.J. Zalewski, S. Alerasool, P.K. Doolin, Catal. Today 53 (1999) 419.
[32] L. Ben Hammouda, Relation entre paramètres de préparation, structure et réactivité de la zircone sulfatée, élaborée par voie sol–gel, PhD Thesis, Université de Tunis El Manar, 2003.
[33] J.A. Moreno Lopera, Improvement of sulfated zirconia catalysts for n-butane isomerization by Al- and Ga-promotion, PhD Thesis, Université catholique de Louvain, 2002.
[34] C.L. Bianchi, S. Ardizzone, G. Cappelletti, Surf. Interface Anal. 36 (2004) 745.
[35] S. Ardizzone, C. Bianchi, G. Cappelletti, F. Porta, J. Catal. 227 (2004) 470.
[36] J. Lilja, J. Warna, T. Salmi, L.J. Pettersson, J. Ahlkvist, H. Grenman, M. Ronnholm, D.Y. Murzin, Chem. Eng. J. 115 (2005) 1–12.